

HD-A136 817

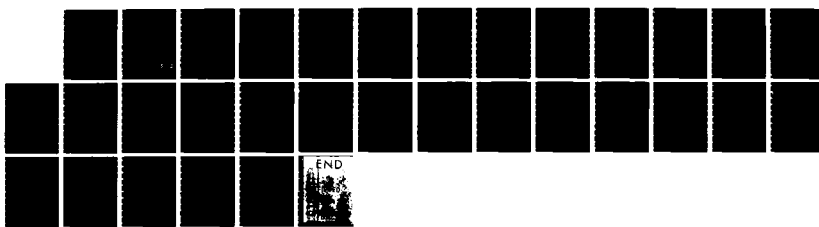
SOURCE REGION EMP COUPLING TO LONG LINES(U) JAYCOR  
SANTA BARBARA CA D F HIGGINS ET AL. 01 JUN 81  
JAYCOR-J200-81-321-2193 DNA-6269F DNA001-80-C-0173

1/1

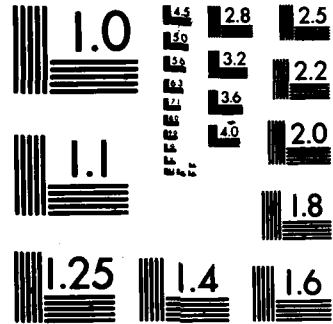
UNCLASSIFIED

F/G 20/14

NL



END



MICROCOPY RESOLUTION TEST CHART  
NATIONAL BUREAU OF STANDARDS-1963-A

AJ-E301291

12

DNA 6269F

AD-A136817

# SOURCE REGION EMP COUPLING TO LONG LINES

JAYCOR  
P. O. Box 30281  
Santa Barbara, California 93130

1 June 1981

Final Report for Period 3 March 1980–1 June 1981

CONTRACT No. DNA 001-80-C-0173

APPROVED FOR PUBLIC RELEASE;  
DISTRIBUTION UNLIMITED.

THIS WORK WAS SPONSORED BY THE DEFENSE NUCLEAR AGENCY  
UNDER RDT&E RMSS CODE B323080464 X99QAXVD40103 H2590D.

DTIC FILE COPY

Prepared for  
Director  
DEFENSE NUCLEAR AGENCY  
Washington, DC 20305

DTIC  
ELECTED  
S JAN 12 1984 D  
B

83 12 09 066

Destroy this report when it is no longer  
needed. Do not return to sender.

PLEASE NOTIFY THE DEFENSE NUCLEAR AGENCY,  
ATTN: STTI, WASHINGTON, D.C. 20305, IF  
YOUR ADDRESS IS INCORRECT, IF YOU WISH TO  
BE DELETED FROM THE DISTRIBUTION LIST, OR  
IF THE ADDRESSEE IS NO LONGER EMPLOYED BY  
YOUR ORGANIZATION.



## UNCLASSIFIED

SECURITY CLASSIFICATION OF THIS PAGE (When Data Entered)

REPORT DOCUMENTATION PAGE		READ INSTRUCTIONS BEFORE COMPLETING FORM
1 REPORT NUMBER DNA 6269F	2 GOVT ACCESSION NO. <i>ADA136 817</i>	3 RECIPIENT'S CATALOG NUMBER
4. TITLE (and Subtitle)  SOURCE REGION EMP COUPLING TO LONG LINES	5 TYPE OF REPORT & PERIOD COVERED Final Report for Period 3 Mar 1980—1 Jun 1981	
7 AUTHOR(s) D.F. Higgins            K.S. Smith T.A. Tumollilo        J.P. Wondra W.A. Radasky	6 PERFORMING ORG REPORT NUMBER J200-81-321/2193	
9. PERFORMING ORGANIZATION NAME AND ADDRESS JAYCOR P.O. Box 30281 Santa Barbara, California 93130	8 CONTRACT OR GRANT NUMBER DNA 001-80-C-0173	
11. CONTROLLING OFFICE NAME AND ADDRESS Director Defense Nuclear Agency Washington, D.C. 20305	10 PROGRAM ELEMENT PROJECT TASK AREA & WORK UNIT NUMBERS Subtask X99QAXVD401-03	
14 MONITORING AGENCY NAME & ADDRESS (if different from Controlling Office)	12 REPORT DATE 1 June 1981	
	13. NUMBER OF PAGES 32	
	15 SECURITY CLASS (of this report) UNCLASSIFIED	
	15a DECLASSIFICATION DOWNGRADING SCHEDULE N/A SINCE UNCLASSIFIED	
16 DISTRIBUTION STATEMENT (of this Report)  Approval for public release, distribution unlimited.		
17. DISTRIBUTION STATEMENT (of the abstract entered in Block 20, if different from Report)		
18. SUPPLEMENTARY NOTES  This work was sponsored by the Defense Nuclear Agency under RDT&E RMSS Code B323080464 X99QAXVD40103 H2590D.		
19 KEY WORDS (Continue on reverse side if necessary and identify by block number) Source Region EMP Long Line EMP Coupling Transmission Line Models Finite-Difference Techniques		
20 ABSTRACT (Continue on reverse side if necessary and identify by block number)  This report compares the results of several calculational techniques used to evaluate the results of source region EMP coupling to long lines. In particular, approximate transmission line models are compared to more detailed three-dimensional finite-difference techniques for both aerial and buried long lines. The two methods are shown to be in fairly good agreement for buried lines, but substantial differences were seen for aerial lines where time-dependent air conductivity is an important factor.		

## SUMMARY

The results discussed in this paper can be summarized as follows:

1. Early time (less than a microsecond) response of aerial lines are apparently highly dependent upon details of the time-dependent air conductivity. Transmission line results do not agree well with finite-difference calculations for this case.
2. For buried cables, early-time results from both transmission line and finite-difference calculations seem to be in fair agreement. This is probably due to partial isolation of the line from the Compton current driver by the conducting ground.
3. Late-time transmission line calculations (for both aerial and buried cables) indicate that large currents may flow at late times. This large current is due to the predicted slow decay of the radial electric field generated by a nuclear burst, combined with a decreasing line impedance as fields diffuse into the ground. As a result, large currents can persist for hundreds of microseconds.
4. Quasi-static analytic solutions for certain cases have also been given. These expressions point out the importance of assumed loads at the end of the line. (A low impedance at each end can result in very large late-time currents.) Such solutions also provide checks of the late-time accuracy of transmission line calculations.

Accession For	
NTIS GRA&I	
DTIC TAB	
Unannounced	
Justification	
By	
Distribution/	
Availability Codes	
Dist	Avail and/or Special
A-1	

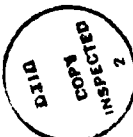


## **TABLE OF CONTENTS**

SUMMARY.....	1
LIST OF ILLUSTRATIONS .....	3
INTRODUCTION.....	5
EARLY-TIME FINITE-DIFFERENCE CALCULATIONS.....	5
TRANSMISSION LINE CALCULATIONS.....	12
REFERENCES.....	24

## LIST OF ILLUSTRATIONS

<b>FIGURE</b>		<b>PAGE</b>
1	Geometry for SREMP coupling to a wire over a ground plane.....	6
2	The normalized Compton current time history $f(t)$ and the peak Compton current density vs. axial position.....	8
3	Peak value of the cable current vs. axial position and time variation of the current on the cable at a few axial positions (arrows on time histories indicate window times at that $z$ location).....	10
4	Conductivity vs. axial position near the cable and between cable and ground.....	11
5	Currents on a buried cable at early times as calculated by FDTD code.....	13
6	Early-time current waveforms as a function of position on an aerial cable as predicted by a transmission line calculation. Geometry is the same as in Figure 1.....	17
7	Currents on a buried cable at early times as calculated by transmission line techniques.....	19
8	Current at the center of a 2000 meter long insulated cable (current at other locations along cable is virtually identical).....	22
9	Currents on a 2000 meter buried cable in good electrical contact with the ground driven by a distributed source..	23

**(THIS PAGE INTENTIONALLY LEFT BLANK)**

## **INTRODUCTION**

It has been recognized for some time that nuclear bursts near or at the air-ground interface can create Compton current densities over a substantial volume. This EMP source region can result in large electromagnetic transients that radiate to far distances. As a result, complex EMP phenomenology codes have been written to calculate the electromagnetic fields.<sup>1-3</sup> Another concern, however, is the coupling of such fields to conductors that may exist inside the source region. Note that such conductors may include telephone or power lines which will not survive the nuclear blast, but are electrically connected to systems outside the source region. A large transient may thus be transmitted to a system of interest, even though the conductor is destroyed.

Calculations of source region coupling to long lines are greatly complicated by the complex three-dimensional geometry, the diversity of length scales (i.e., line cross-sectional dimensions vs. length), and the non-linear air conductivity effects. Many previous source region coupling calculations<sup>4-7</sup> have used time-domain transmission line models driven by the output of two-dimensional EMP phenomenology codes. In recent years, however, three-dimensional, finite-difference codes<sup>8</sup> have been developed that can be used to calculate at least the early-time response of long conductors inside the nuclear source region. Such techniques include various non-linear effects that are missing in transmission line models. This report presents a comparison of such coupling calculations.

## **EARLY-TIME FINITE-DIFFERENCE CALCULATIONS**

Source region coupling is basically an extension of surface burst EMP generation theory. Compton currents are used as drivers for finite-difference approximations of the two time-dependent Maxwell equations,

while the air ionization rate (which is proportional to the Compton current at sea level air densities) is used in simplified air chemistry reaction-rate equations to calculate the time-dependent electron and ion densities. These densities are then combined with field-dependent expressions for the mobility to obtain a time-varying conductivity, which is used in Maxwell's equations. Details of this theory have been discussed elsewhere,<sup>1</sup> and will thus not be repeated here. Note, however, that such calculations are non-linear primarily due to the field-dependent mobility.

Unfortunately, adding even a radial-directed wire to a surface burst EMP calculation destroys the usually assumed 2-D symmetry and greatly increases the numerical complexity. At early times (less than about a microsecond), however, the high air conductivity makes the problem primarily a local one in that the Compton currents in a small volume around the conductors generate the fields which are responsible for currents on the conductors. In this time regime, 3-D finite-difference time-domain (FDTD) calculations are possible, although special techniques are required to reduce computer costs to reasonable values.

As an example, the PRES-3D computer code<sup>8</sup> was used to calculate SREMP coupling to the aerial wire geometry shown in Figure 1. The weapon

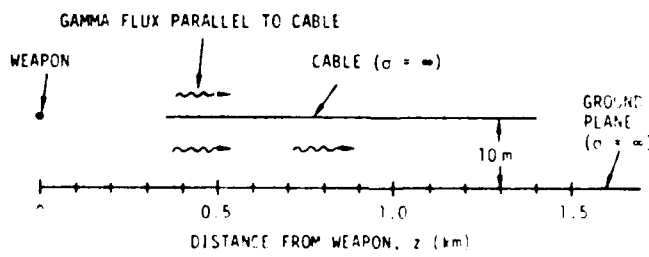


**Figure 1. Geometry for SREMP coupling to a wire over a ground plane.**

2

is assumed to be detonated approximately 350 m away from the cable and on the axis of the cable. The cable length was selected to be long enough to allow observation of current propagation, but was limited by computer cost considerations. The cable was placed 10 meters above a perfectly conducting ground. The gamma-flux was assumed to be parallel to the cable. At a point  $z$  meters from the weapon and  $t$  seconds after detonation, the Compton current  $J_z(z,t)$  and air ionization rate  $S(z,t)$  in the vicinity of the cable were prescribed as

$$J_z(z,t) = 3.4 \times 10^{10} \frac{\exp(-z/320)}{z^2} f(t-z/c) \text{ (A/m}^2\text{)} , \quad (1)$$

$$S(z,t) = 8.2 \times 10^{22} J(z,t) \text{ (ion pairs/m}^3/\text{s)}^9 . \quad (2)$$

The time history,  $f(t)$ , and the peak Compton current versus axial position are displayed in Figure 2. The rise time of the current density and the cable dimensions force grid sizes for the finite-difference solution to be on the order of 10 cm to 1 m. For a cable about 1 km in length, many millions of such points would be required to solve the finite-difference equations in the entire volume. This is not practical on existing computers. If the cylindrical wire is perfectly conducting, any induced fields will be propagated along the wire axis with a velocity determined solely by the external medium. Thus, to examine the prompt fields on the wire, it is not necessary to model the entire cable for all times, but only a small fraction of the cable length which encompasses the Compton current pulse and which moves along the wire with the pulse.

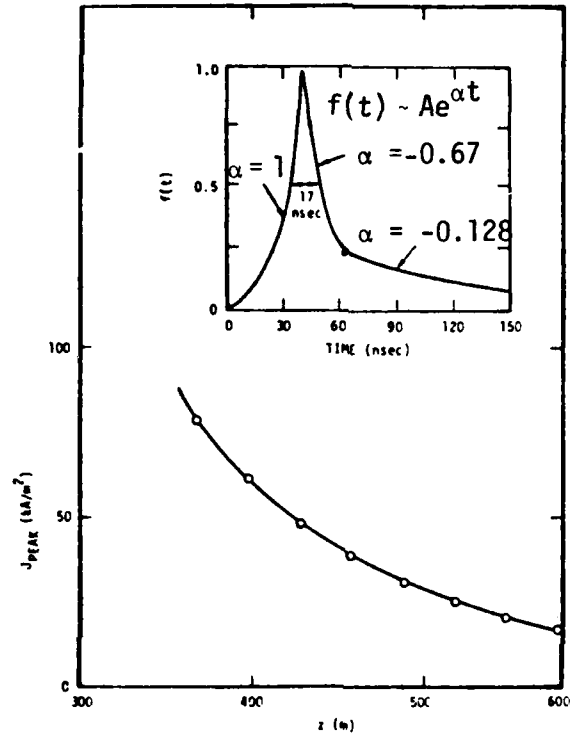


**Figure 2.** The normalized Compton current time history  $f(t)$  and the peak Compton current density vs. axial position.

One thus has a "moving window" simulation volume which propagates down the wire at the velocity of the driver. Such a technique enables one to include many of the advantages of a retarded time calculation in a real time computer code. Also, using this method, and one plane of symmetry through the wire, reduces the number of grid points to a manageable level.

For this problem, the moving simulation volume was 75 m along the axis of the wire. This problem has a plane of symmetry in a vertical

plane through the wire center, which reduced the number of required mesh points by a factor of 2. The zoning along the y axis was carried out to 31 m from wire center. Along x (vertical), there was 10 m between wire and ground and 21 m between the wire and the top of the simulation volume. All boundaries of the simulation volume had perfectly conducting boundary conditions. The use of this boundary condition for the ground was intentional to allow comparisons between this calculation and other models. It is expected that the highly conducting air during the gamma pulse will not allow the other artificial boundary conditions to affect the results for our short timeframe of interest in this calculation. The moving simulation volume used 67,000 zones. The zoning along the z axis necessary to resolve the propagating source was a constant 1.5 m. Along the x and y axes, the zoning was 11 cm in the vicinity of the wire and was gradually extended to several meters at the extreme of the simulation volume.

The Compton currents were defined at the mesh points using the analytical formula of Equation (1). The ionization rate of Equation (2) was used as the source term for the three-species air-chemistry equations. The solutions between the field equations and the air-chemistry equations were done self-consistently--i.e., the air-chemistry parameters and conductivity are field-dependent and, similarly, the field solutions depend strongly on the conductivity.

To anticipate some of the results of the simulation, it was observed that neither the perfectly conducting boundary conditions nor the large cells at the end points appeared to have any influence on the current carried by the wire. This is no doubt due to the very long path that any EM wave must transverse through an ionized conducting medium from a boundary to the wire.

Figure 3 displays the peak value of the cable current as a function of axial position along the wire. Time histories of the current at several points along the wire are also displayed in this Figure. The current waveform rises rapidly ( $\sim 40$  nsec), then tends to be relatively constant for about 100 nsec, and then starts to decay.

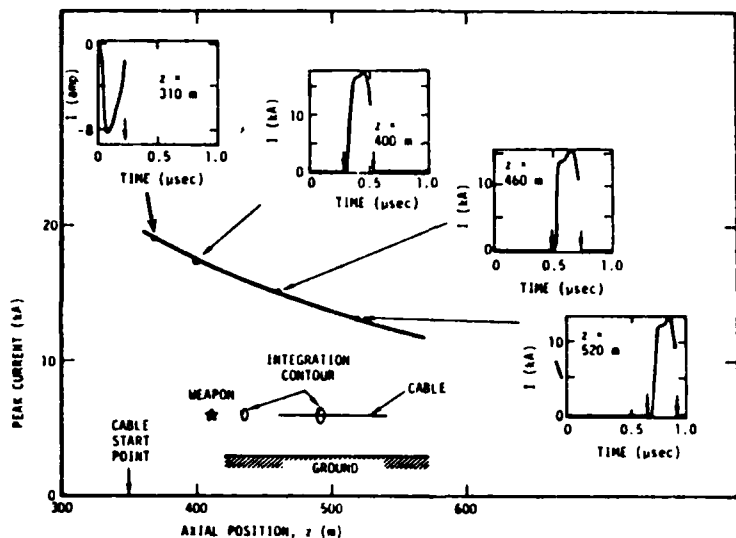


**Figure 3.** Peak value of the cable current vs. axial position and time variation of the current on the cable at a few axial positions (arrows on time histories indicate window times at that  $z$  location).

Figure 4 displays the peak value of the air conductivity versus axial position for a point near the cable and a point between the cable and ground. Note that the conductivity is significantly higher near the cable because, as we approach the cable (or the ground), the boundary conditions require that the tangential electric field be zero on the cable and ground. The lower field values near the ground and the wire give much

higher electron mobilities and, hence, a higher conductivity. (Zero water vapor content was assumed in these calculations.)

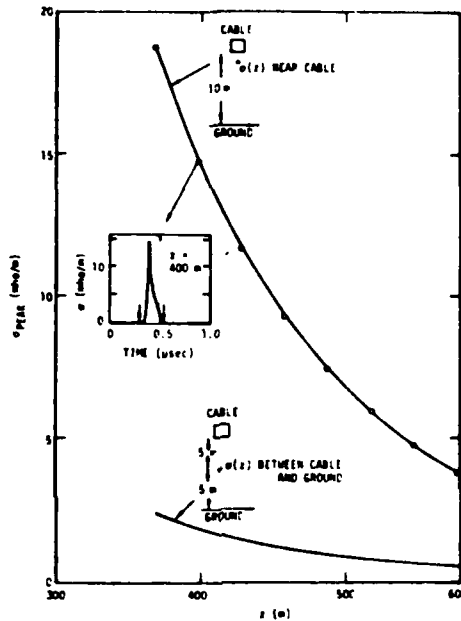


**Figure 4. Conductivity vs. axial position near the cable and between cable and ground.**

Note that the aerial cable of this calculation is 10 centimeters in diameter and is uninsulated. The high conductivity near its surface thus makes it possible for large currents to flow on or off the cable. The situation might be even more complicated if the wire were very thin because large perpendicular electric fields would exist at the surface of the wire, perhaps reducing the conductivity there. At a few centimeters from the surface, however, fields would be small, giving an enhanced conductivity. In any case, the air conductivity in any plane perpendicular to the axis of the long conductor is apparently not uniform (a fact often assumed in simpler models).

As a second example, finite-difference time-domain techniques were used to calculate the response of an insulated, buried cable. The cable was 10 meters in length and was buried one meter below the ground-air interface. The ground conductivity was assumed to be  $10^{-3}$  mho/m and the dielectric constant was  $6\epsilon_0$ . The conducting cable was 1/4 inch in diameter, and, for these calculations the source term was a prescribed electric field along the air-ground interface above the cable. The time history of this field was triangular, rising to a peak of 100 kV/m in 5 nsec, and then returning to zero at 300 nsec. The starting time of this prescribed surface field was phased at the speed of light along the cable. Some sample results for this example are shown in Figure 5. As before, calculations are limited to early times by the expenses of computer time.

#### **TRANSMISSION LINE CALCULATIONS**

Transmission line modeling<sup>10-13</sup> is a fairly well established method for calculating EMP coupling to long conductors that are outside of the nuclear source region. Such methods are also used for coupling inside the source region, but the adequacy of such methods is rather uncertain under such conditions (especially at early times).

Transmission line techniques have the great advantage of being capable of calculating late-time response of very long conductors at a reasonable cost. Such late-time response calculations are believed to be very important because EMP generation models indicate that substantial late-time electric fields are produced by a surface-level nuclear burst. The apparent result is very large amounts of late-time (~1 millisecond) EM energy coupled to long lines.

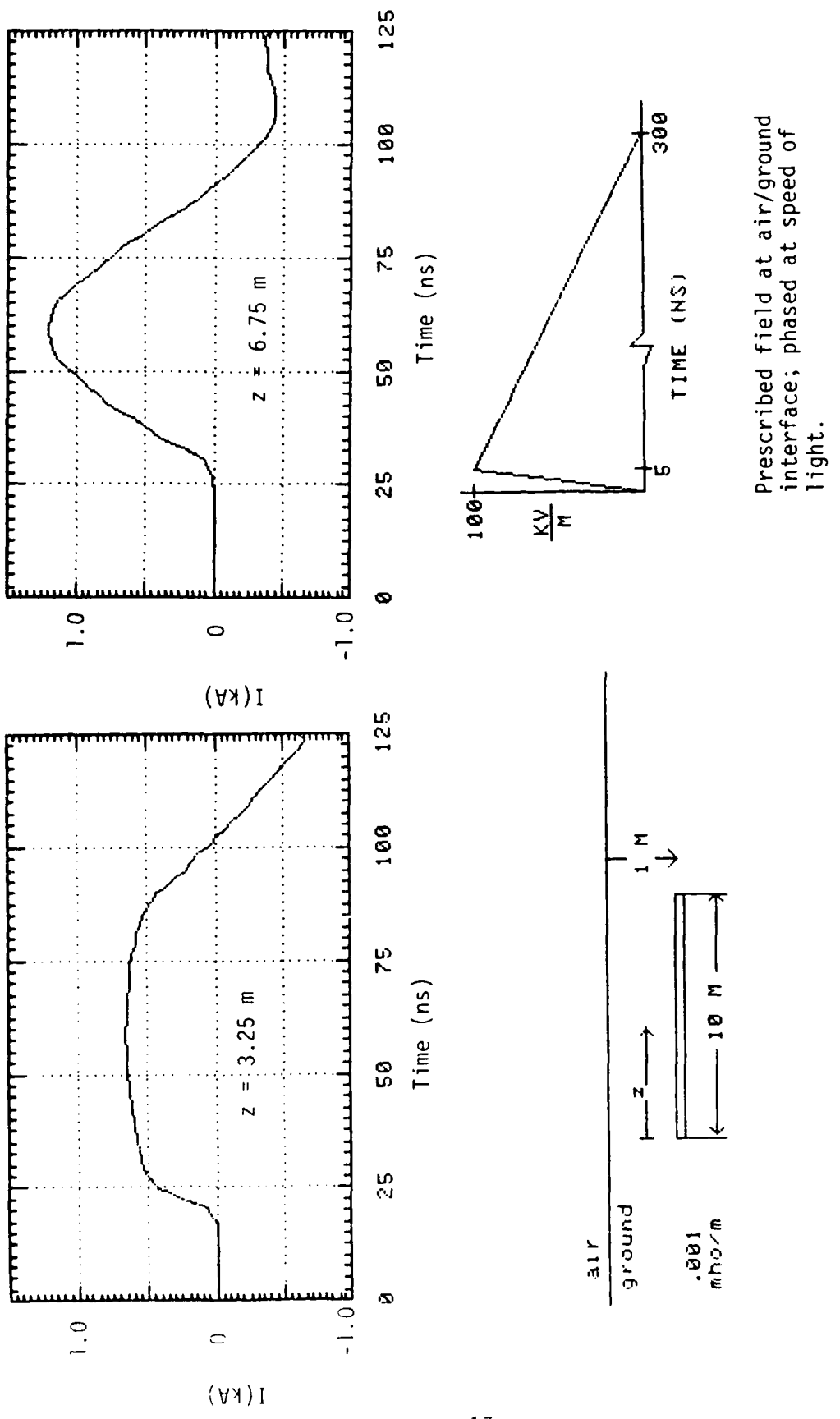


Figure 5. Currents on a buried cable at early times as calculated by FDTD code.

The time-dependent transmission line equations can be written<sup>10</sup> as

$$L \frac{\partial I}{\partial t} + RI = V_D - \frac{\partial V}{\partial z} \quad (3)$$

and

$$C \frac{\partial V}{\partial t} + GV = - \frac{\partial I}{\partial z} \quad (4)$$

where  $I$  and  $V$  are the current and voltage along the line;  $L$ ,  $C$ ,  $R$  and  $G$  are respectively the inductance, capacitance, resistance, and conductance per-unit-length of the line and  $V_D$  is the per-unit-length voltage source driver. The driver,  $V_D$ , is usually assumed equal to the electrical field along the wire if the wire was absent (i.e., the incident electric field).

Note that in many special cases, one can obtain analytic solutions for the current and voltages along the line. Numerical solutions are also straightforward and with implicit-differencing techniques, solutions can be obtained over long time periods. The primary problem in using transmission line theory is thus determining the proper expressions for four line parameters  $L$ ,  $C$ ,  $R$  and  $G$ .

In some cases, appropriate line parameters are well known.<sup>11</sup> If one assumes an aerial conductor of diameter  $d$  at a height  $h$  above a perfectly conducting ground plane, then

$$L = \frac{\mu_0}{2\pi} \cosh^{-1} \left( \frac{2h}{d} \right) \quad (5)$$

and

$$C = \frac{2\pi\epsilon_0}{\cosh^{-1}\left(\frac{2h}{d}\right)} \quad (6)$$

while if the region between the wire and the ground has a uniform conductivity,  $\sigma$ , then

$$G = \frac{2\pi\sigma}{\cosh^{-1}\left(\frac{2h}{d}\right)} \quad . \quad (7)$$

For this example, currents will flow in one direction along the aerial wire and return through the ground plane, with some leakage through the intervening conducting media. For a perfectly conducting ground, the resistance per unit length is zero.

One approach is to simply use these expressions with a time-dependent conductivity in Equation (7), thus giving a time-dependent conductance. The conductivity to be used might be that calculated by a 2-D EMP code which does not include the wire. (Such a calculation also provides the per unit length voltage source,  $V_D$ .)

Such an approach does not include the fact that at early times in the source region, air conductivities become large enough to isolate an aerial conductor from the local ground. Return currents will then flow through the conducting air, rather than on the ground plane.

An empirical method for attempting to include this effect<sup>6</sup> is to define a time-dependent skin depth in the air,  $\delta(t)$ , where

$$\delta(t) = \sqrt{\frac{2t}{\mu_0 \sigma(t)}} \quad . \quad (8)$$

When  $\delta(t) < h$ , it can be assumed that return currents flow through the air within a distance  $\delta$  of the wire.

One then uses the coaxial formulas<sup>11</sup>

$$L = \frac{\mu_0}{2\pi} \ln \left( \frac{2\delta(t)}{d} \right) \quad (9)$$

$$C = \frac{2\pi\epsilon_0}{\ln \left( \frac{2\delta(t)}{d} \right)} \quad (10)$$

$$G = \frac{2\pi\sigma(t)}{\ln \left( \frac{2\delta(t)}{d} \right)} \quad (11)$$

$$R = \frac{1}{\sigma(t)\pi\delta^2(t)} \quad . \quad (12)$$

On the other hand, when the skin depth becomes larger than the wire height above the ground, the previous expressions for the line parameters are applicable.

Some representative results of a transmission line calculation using these expressions are shown in Figure 6. In this case, the assumed geometry is identical to that previously used in the finite-difference calculations (see Figure 1) while the time-dependent source term,  $V_D$ , and conductivity,  $\sigma(t)$  used in the transmission line calculation were taken from the finite-difference results (at a point distant from the aerial conductor).

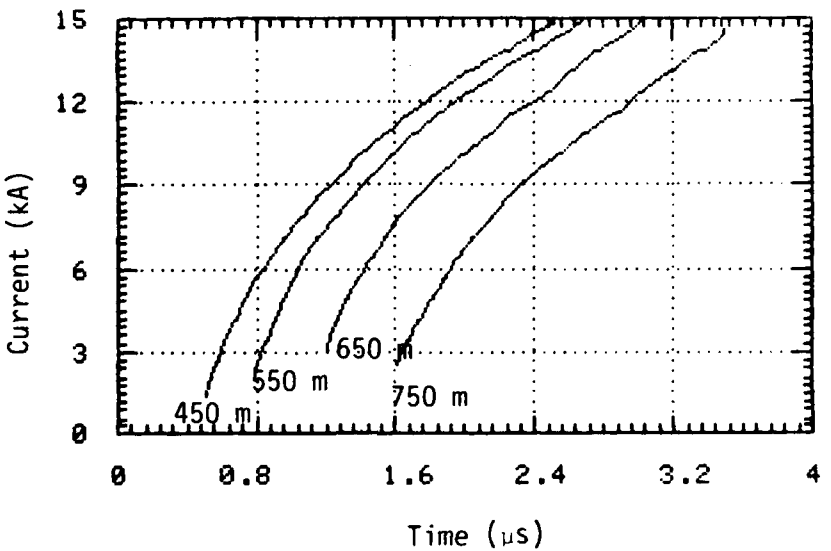


**Figure 6. Early-time current waveforms as a function of position on an aerial cable as predicted by a transmission line calculation. Geometry is the same as in Figure 1.**

A comparison of these transmission line results with those previously obtained using finite-difference techniques shows little agreement. Transmission line currents rise relatively slowly but continually over the time period calculated, compared to the early time peaks seen in the finite-difference calculations. However, one would somewhat expect the transmission line calculations to be incorrect at early times because many approximations and assumptions inherent to such models are clearly invalid. For example, the air conductivity in any plane perpendicular to the conductor was assumed to be independent of location, an assumption that is demonstrated to be incorrect by the finite-difference results of Figure 4.

Transmission line techniques may be more applicable for a buried conductor, however, where the local conductivity is fairly uniform and does not vary with time. Fields generated by Compton currents in the air diffuse into the ground to drive the cable, while return currents must also flow through the conducting soil. Again one can use the concept of a time-dependent skin-depth

$$\delta_g(t) = \sqrt{\frac{2t}{\mu_0 \sigma_g}} \quad (13)$$

where  $\sigma_g$  is the ground conductivity. As before, this results in time-dependent transmission line parameters (see Equations (9) through (12)). However, L, C and G have only a logarithmic time dependence, while the resistance per unit length, R, is approximated by

$$R \approx \frac{1}{\pi \sigma_g \delta_g^2(t)} = \frac{\mu_0}{2\pi t} \quad . \quad (14)$$

The resistance of the current return path through the ground thus decreases linearly with time.

Results of a transmission line model of coupling to a 10 meter long cable buried one meter deep are shown in Figure 7. Problem parameters are the same as previously discussed with the comparable finite-difference calculation. A comparison of these results with those previously shown in Figure 5 indicates a reasonable agreement between the simple transmission line calculation and finite-difference results. Predicted waveforms have quite similar shapes, although magnitudes differ by about a factor of two.

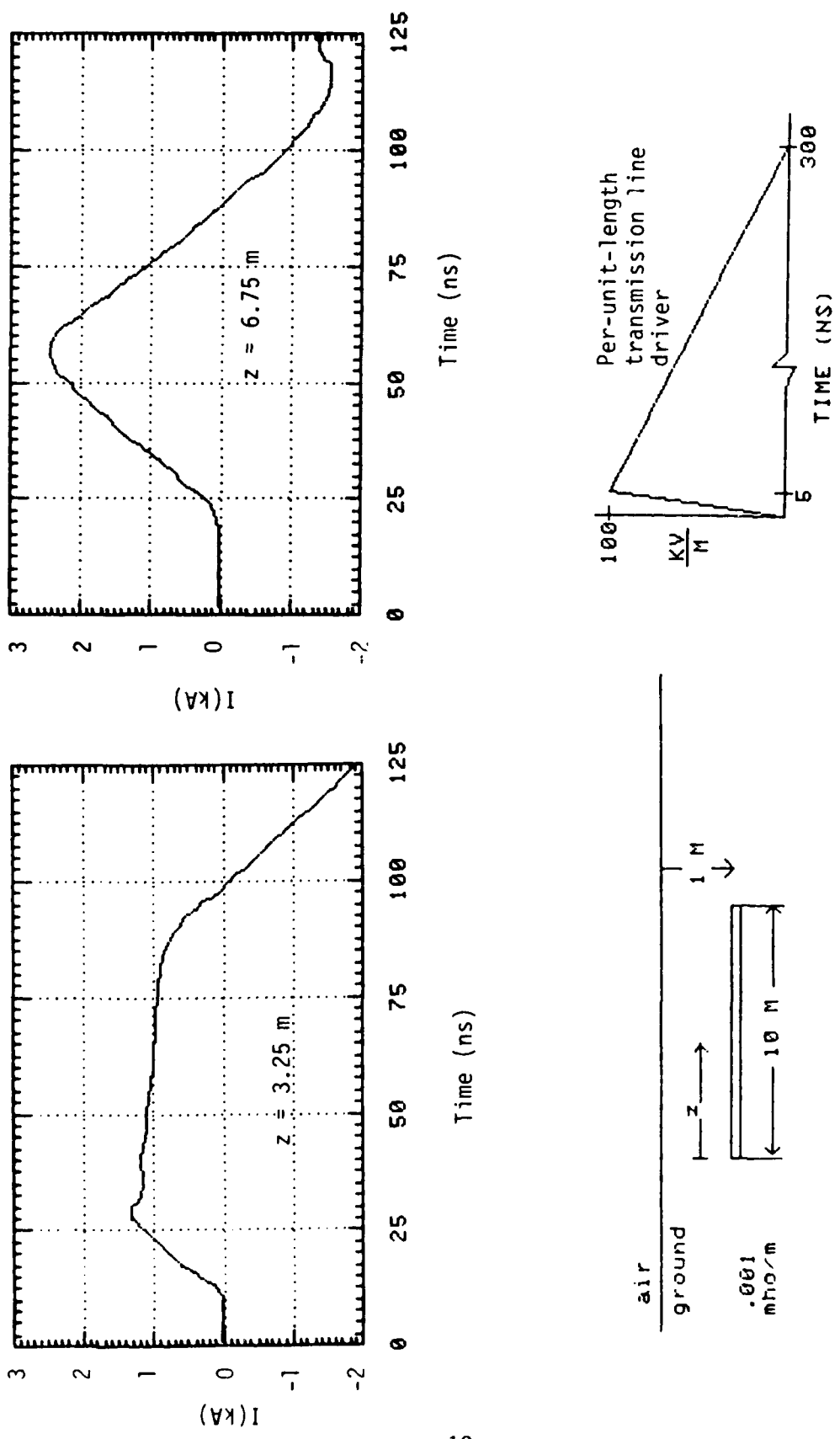


Figure 7. Currents on a buried cable at early times as calculated by transmission line techniques.

Consider now a long buried conductor and its SREMP response at late times (i.e., times of roughly 1 millisecond). Finite-difference time-stepping calculations cannot practically be carried out to such late times, but transmission line methods can be. Fortunately, such results at late times can be checked against certain analytic calculations or circuit models.

As an example, consider a conductor (either buried or in the air) of length  $\ell$  (where  $\ell$  may be of the order of 1-2 kilometers). If late-time SREMP fields are slowly changing, skin depths and wavelengths are greater than or equal to cable lengths. Equation (14) indicates that the resistance per unit length of the line is small, as is the inductive impedance at late times. For an insulated line, the late-time current then depends primarily on the loads at the ends of the conductor. If  $E_0$  is the average incident electric field along the conductor, and  $R_1$  and  $R_2$  are resistive loads at each end, then the late-time current is approximated by

$$I = \frac{E_0 \ell}{R_1 + R_2 + R\ell} \quad (15)$$

as is readily seen by a simple equivalent circuit model. If such a line runs radially outward from a nuclear fireball, the load  $R_1$  may be quite small (i.e., the line is shorted to ground by the conducting fireball). The current at late times is thus primarily limited by the load at the far end,  $R_2$ . EMP environment codes indicate that substantial electric fields may exist at late times. For example, an  $E_0$  of even 100 v/m over a kilometer of cable gives a voltage source of  $10^5$  volts and if  $R_2$  is about 100 ohms, late-time currents of 1000 amps will be generated.

If a cable is uninsulated, late-time results are slightly more complicated because current can leak off the cable along its entire length. However, in the static limit, when a uniform driver is applied to an uninsulated transmission line, one can show that the spatial current is given by

$$I(z) = \frac{E_0}{R} - \sqrt{\frac{G}{R}} \left\{ A \exp(\sqrt{RG}z) - B \exp(-\sqrt{RG}z) \right\} \quad (16)$$

where  $A$  and  $B$  are constants which depend upon the loads at each end of the line (i.e.,  $A$  and  $B$  are determined by the boundary conditions). For example, with resistive loads  $R_1$  and  $R_2$ , where  $R_1=0$ , then  $A=-B$  and one can show that

$$A = \frac{E_0 R_2 / R}{R_2 \sqrt{\frac{G}{R}} e^{\xi} + e^{-\xi} + e^{\xi} - e^{-\xi}} \quad (17)$$

where  $\xi = \sqrt{RG}\ell$  and  $\ell$  is the length of the line. This solution indicates that there is a characteristic length at late times given by  $(RG)^{-1/2}$ .

Late-time transmission line calculations can thus be checked against such specific analytic solutions. As an example, consider a 2000 meter long cable, buried in  $10^{-3}$  mho/m soil, driven by the field

$$E_0(\tau) = 100(\tau/T)^{-1/2} \text{ V/m} \quad (18)$$

where

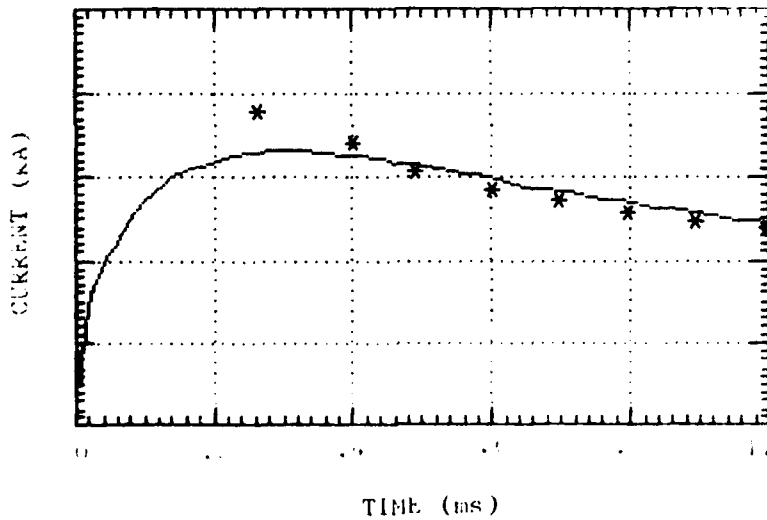
$$\tau = \text{retarded time} = t - z/c$$

and

$$T = 10^{-3} \text{ sec} .$$

Transmission line calculations of the resulting cable currents for insulated and uninsulated lines are shown in Figures 8 and 9. A comparison of these results at late-times with the analytic expressions in Equations (15) and (16) indicate that the transmission line results do indeed approach the analytic expressions for the static limits.

It is also interesting to note that currents along most of the length of the uninsulated wire exceed those on the insulated wire. At the far end (at  $R_2$ ), however, the current is smaller for the uninsulated case than for the insulated line.



**Line Parameters:**

$l = 2000 \text{ m}$

$R_1 = 1 \text{ ohm}$

$R_2 = 10 \text{ ohms}$

Solid line - transmission line results

\* - prediction of quasi-static analytic theory

**Driver:**

$E_0(\tau) = 100 (\tau/T)^{-1/2} \text{ V/m}$

$T = 10^{-3} \text{ s}$

**Figure 8.** Current at the center of a 2000 meter long insulated cable (current at other locations along cable is virtually identical).

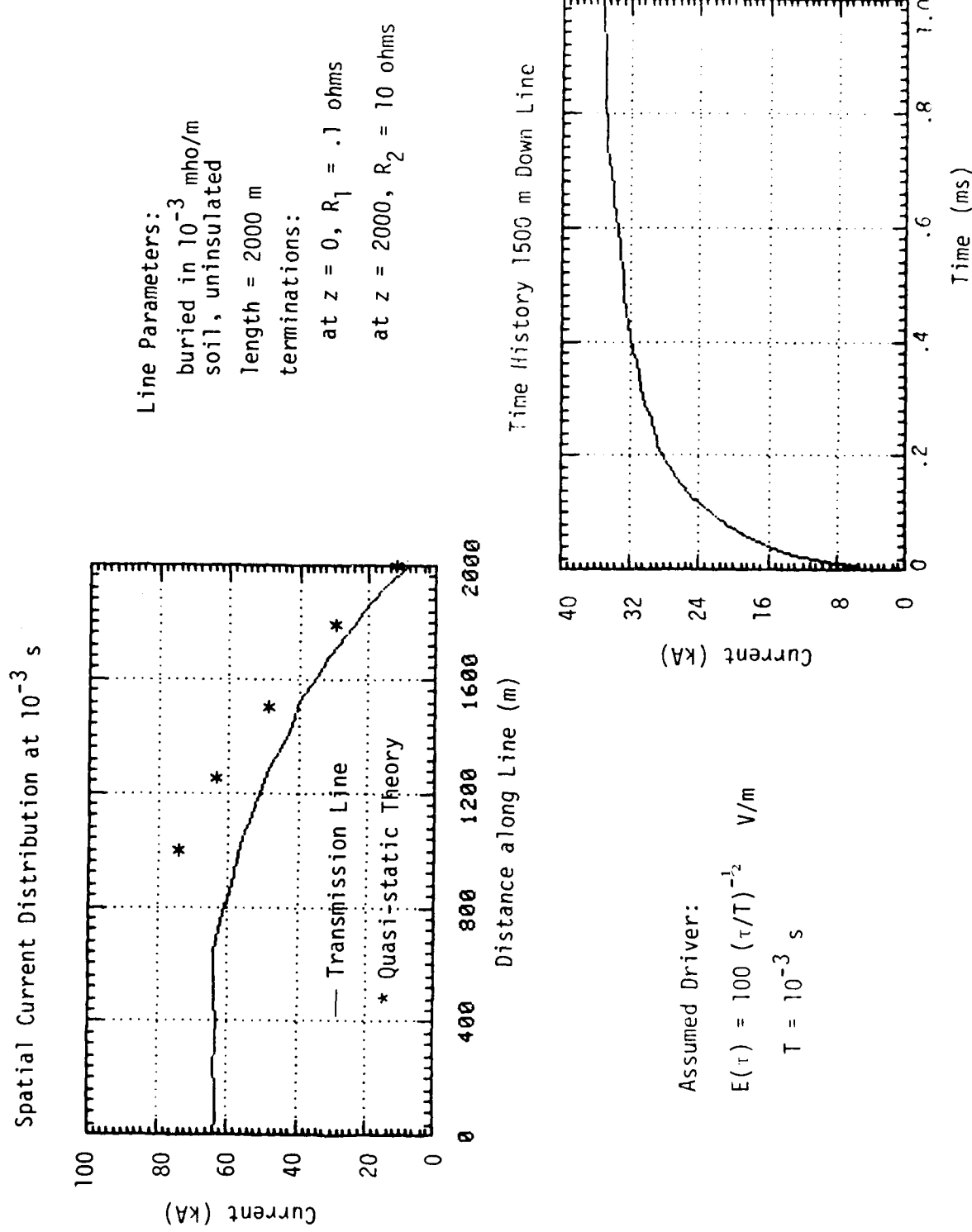


**Figure 9.** Currents on a 2000-meter buried cable in good electrical contact with the ground driven by a distributed source.

## REFERENCES

1. Longmire, C.L., "On The Electromagnetic Pulse Produced by Nuclear Explosions," IEEE Transactions on Antennas and Propagation, Vol. AP-26, No. 1, January 1978.
2. Crevier, W.F., E. Pettus, "Approximate Methods for Calculating the Early Time EMP From Surface Bursts at the Ground in and Near the Source Region," IEEE Transactions on Nuclear Science, Vol. NS-26, No. 6.
3. Grover, M.K., "Some Analytic Models for Quasi-Static Source Region EMP: Application to Nuclear Lightning," IEEE Transactions on Nuclear Science, Vol. NS-28, No. 1, February 1981.
4. Trybus, P.R., A.M. Chodorow, "MLTRANS: A Time-Domain Solution of The Response of Transmission Lines in a Photon Environment," IEEE Transactions on Nuclear Science, Vol. NS-23, No. 6, December 1976.
5. Holland, R., "The EMP Tunnel Code DHTRANS," IEEE Transactions on Nuclear Science, Vol. NS-25, No. 6, December 1978.
6. Perala, R.A., S.R. Rogers, "The Effects of Corona on the EMP Response of Insulated Cables Lying on the Surface of the Earth," IEEE Transactions on Nuclear Science, Vol. NS-27, No. 6, December 1980.
7. Perala, R.A., R.B. Cook, "The Effects of Dielectric and Soil Nonlinearities on the Electromagnetic Transient Response of Cables Lying on the Surface of the Earth," IEEE Transactions on Nuclear Science, Vol. NS-26, No. 6, December 1979.
8. Tumolillo, T.A., et al., "PRES-3D: A Computer Code for SelfConsistent Solution of Maxwell-Lorentz Three-Species Air Chemistry Equations in Three Dimensions," IEEE Transactions on Nuclear Science, Vol. NS-24, No. 6, December 1977.

9. Merewether, D.E., W.A. Radasky, "Non-Linear Electromagnetic Fields Within a Cylindrical Cavity Excited by Ionizing Radiation," IEEE Transactions on Nuclear Science, Vol. NS-21, No. 1, February 1974.
10. Vance, E.F., Coupling to Shielded Cables, John Wiley & Sons, 1978.
11. Ramo, S., J.R. Whinnery, T. Van Duzer, Fields and Waves in Communication Electronics, John Wiley & Sons, New York 1965.
12. Lee, K.S.H., "Two Parallel Terminated Conductors in External Fields," IEEE Transactions on Electromagnetic Compatibility, Vol. EMC-20, May 1978.
13. Agrawal, A.K., H.J. Price, S.H. Gurbaxani, "Transient Response of Multiconductor Transmission Lines Excited by a Nonuniform Electromagnetic Field," IEEE Transactions on Electromagnetic Compatibility, Vol. EMC-22, No. 2, May 1980.

## DISTRIBUTION LIST

### DEPARTMENT OF DEFENSE

Assistant to the Secy of Def  
Atomic Energy  
ATTN: Executive Asst  
ATTN: Military Applications

Defense Communications Agency  
ATTN: Code 312  
ATTN: Code C313

Defense Communications Engineer Ctr  
ATTN: Code R123  
ATTN: Code R720, C. Stansberry  
ATTN: Code R400

Defense Intelligence Agency  
ATTN: RTS-2A  
ATTN: DB 4C2, D. Spohn

Defense Nuclear Agency  
ATTN: NATA  
ATTN: STNA  
ATTN: RAEV  
2 cy ATTN: RAEE  
4 cy ATTN: TITL

Defense Tech Info Ctr  
12 cy ATTN: DD

Field Command  
DNA Det 1  
Lawrence Livermore Lab  
ATTN: FC-1

Field Command  
Defense Nuclear Agency  
ATTN: FCPR  
ATTN: FCTT  
ATTN: FCTXE  
ATTN: FCLMC, H. Putnam  
ATTN: FCTT, G. Ganong  
ATTN: FCTT, W. Summa

Interservice Nuclear Weapons School  
ATTN: TTV

Joint Chiefs of Staff  
ATTN: J-3

### DEPARTMENT OF THE ARMY

BMD Systems Command  
ATTN: BMDSC-AOLIB  
ATTN: BMDSC-HLE, R. Webb

Research & Dev Center  
ATTN: DRDCO-SEI  
ATTN: DRCPM-ATC

US Army Communications Command  
ATTN: CC-OPS-PD  
ATTN: ATSI-CD-MD  
ATTN: CC-LOG-LEO  
ATTN: CC-OPS-OS

US Army Engineer Div, Huntsville  
ATTN: HNDED-SR

### DEPARTMENT OF THE ARMY (Continued)

US Army Nuclear & Chemical Agency  
ATTN: MONA-WE

Harry Diamond Labs  
ATTN: DELHD-NW-E  
ATTN: OO100, Commander, Tech Dir, Div Dir  
ATTN: DELHD-NW-EB  
ATTN: DELHD-NW-ED  
ATTN: NWPO  
ATTN: DELHD-R  
ATTN: DELHD-NW, J. Bombardt  
ATTN: DELHD-NW-EE  
ATTN: DELHD-TD  
ATTN: DELHD-NW-EC  
ATTN: DELHD-NW-EA  
ATTN: DELHD-TF  
ATTN: DELHD-NW-P  
ATTN: DELHD-TA-L  
2 cy ATTN: DELHD-NW-RC

DEPARTMENT OF THE NAVY

Naval Ocean Systems Center  
ATTN: Code 54, C. Fletcher  
ATTN: Code 08, J. Rockway  
ATTN: Code 7309, R. Greenwell

Naval Postgraduate School  
ATTN: Code 1424, Library

Naval Research Lab  
ATTN: Code 2627, D. Folen  
ATTN: Code 1434, E. Brancato  
ATTN: Code 4700, W. Ali  
ATTN: Code 2000, J. Brown  
ATTN: Code 5623, R. Statler  
ATTN: Code 6750  
ATTN: Code 4701, I. Vitokovitsky  
ATTN: Code 6624  
ATTN: Code 4760, R. Grieg

Naval Surface Weapons Ctr  
ATTN: Code F-56

Naval Surface Weapons Ctr  
ATTN: Code F32, E. Rathbun  
ATTN: Code F30

DEPARTMENT OF THE AIR FORCE

Air Force Weapons Lab  
ATTN: NTYEE, C. Baum  
ATTN: NTYC, M. Schneider  
ATTN: CA  
ATTN: NXS  
ATTN: NTYEP, W. Page  
ATTN: NT  
ATTN: SUL  
ATTN: NTN

Ballistic Missile Office  
ATTN: ENSN, W. Wilson  
ATTN: ENSN, W. Clark  
ATTN: M. Stapanian  
2 cy ATTN: ENSL

DEPARTMENT OF THE AIR FORCE (Continued)

Air University Library  
ATTN: AUL-LSE

Air Logistics Command  
ATTN: OO-ALC/MMEDO, L. Kidman  
ATTN: OO-ALC/MMETH, P. Berthel  
ATTN: OO-ALC/MM

OTHER GOVERNMENT AGENCY

Central Intelligence Agency  
ATTN: OSWR/NED

DEPARTMENT OF ENERGY CONTRACTORS

University of California  
Lawrence Livermore National Lab  
ATTN: L-10, H. Kruger  
ATTN: L-13, D. Meeker  
ATTN: L-156, H. Cabayan  
ATTN: L-97, T. Donich  
ATTN: L-153, E. Miller  
ATTN: Tech Info Dept Library

Sandia National Labs  
ATTN: C. Vittitoe  
ATTN: T. Martin  
ATTN: R. Parker  
ATTN: G. Yonas  
ATTN: Org 9336, E. Hartman

DEPARTMENT OF DEFENSE CONTRACTORS

BDM Corp  
ATTN: Corporate Library  
ATTN: S. Clark  
ATTN: W. Sweeney

American Telephone & Telegraph Co  
ATTN: W. Edwards

BDM Corp  
ATTN: Library

Boeing Co  
ATTN: Kent Tech Library  
ATTN: D. Kemle  
ATTN: H. Wicklein  
ATTN: B. Hanrahan

Dikewood  
ATTN: Tech Lib for C. Jones  
ATTN: Tech Library  
ATTN: Tech Lib for D. Pirio

Dikewood Corporation  
ATTN: K. Lee

EG&G Wash Analytical Svcs Ctr, Inc  
ATTN: C. Giles

Electro-Magnetic Applications, Inc  
ATTN: D. Merewether

General Electric Co  
ATTN: J. Andrews  
ATTN: D. Nepveux  
ATTN: J. Peden

DEPARTMENT OF DEFENSE CONTRACTORS (Continued)

GTE Communications Products Corp  
ATTN: D. Flood  
ATTN: C. Ramsbottom  
ATTN: J. Concordia  
ATTN: J. Waldron  
ATTN: A. Novenski  
ATTN: I. Kohlberg  
ATTN: C. Thornhill

IRT Corp  
ATTN: N. Rudie  
ATTN: B. Williams

JAYCOR  
4 cy ATTN: D. Higgins  
4 cy ATTN: W. Radasky  
4 cy ATTN: T. Tumolillo  
4 cy ATTN: K. Smith  
4 cy ATTN: J. Wondra

JAYCOR  
ATTN: E. Wenaas  
ATTN: R. Stahl

JAYCOR  
ATTN: Library

Kaman Sciences Corp  
ATTN: N. Beauchamp  
ATTN: F. Shelton  
ATTN: A. Bridges  
ATTN: W. Rich

Kaman Tempo  
ATTN: DASIAC  
ATTN: W. McNamara  
ATTN: R. Rutherford  
ATTN: W. Hobbs Jr

Kaman Tempo  
ATTN: DASIAC

Martin Marietta Corp  
ATTN: J. Casalese  
2 cy ATTN: M. Griffith

McDonnell Douglas Corp  
ATTN: S. Schneider  
ATTN: Tech Library Svcs

Mission Research Corp  
ATTN: EMP Group  
ATTN: W. Crevier  
2 cy ATTN: C. Longmire

Mission Research Corp  
ATTN: A. Chodorow  
ATTN: M. Scales

Mission Research Corp, San Diego  
ATTN: B. Passenhein

Mission Research Corporation  
ATTN: W. Ware  
ATTN: W. Stark  
ATTN: J. Lubell

Pacific-Sierra Research Corp  
ATTN: H. Brode, Chairman Sage  
ATTN: L. Schlessinger

DEPARTMENT OF DEFENSE CONTRACTORS (Continued)

R&D Associates

ATTN: C. Mo  
ATTN: M. Grover  
ATTN: W. Karzas  
ATTN: Document Control  
ATTN: W. Graham  
ATTN: P. Haas

Rand Corp

ATTN: P. Davis  
ATTN: W. Sollfrey  
ATTN: Lib-D

Rand Corp

ATTN: B. Bennett

Raytheon Co

ATTN: H. Flescher  
ATTN: M Nucefora

IIT Research Institute

ATTN: I. Mindel  
ATTN: J. Bridges

DEPARTMENT OF DEFENSE CONTRACTORS (Continued)

Science & Engrg Associates, Inc  
ATTN: V. Jones

Science Applications, Inc  
ATTN: W. Chadsey

SRI International  
ATTN: A. Whitson  
ATTN: E. Vance

Teledyne Brown Engineering  
ATTN: F. Leopard  
ATTN: J. Whitt

TRW Electronics & Defense Sector  
ATTN: H. Holloway

ATTN: O. Adams  
ATTN: R. Plebuch  
ATTN: L. Magnolia  
ATTN: W. Gargaro

GTE Communications Products Corp  
ATTN: L. Blaisdell

END

FILMED

2-84

DTIC